Scattering of 37-Mev Positive Pions on Hydrogen*

A. M. SACHS, H. WINICK, AND B. A. WOOTEN†
Nevis Cyclotron Laboratory, Columbia University, Irvington-on-Hudson, New York
(Received August 26, 1957)

Measurements have been made of the differential scattering cross sections of positive pions on hydrogen at 37 Mev using a liquid hydrogen target and scintillation counters. Scattered pions are separated from other particles in the background by measuring the mass and energy of the particles using a pulse-height analysis on the signals from the scintillation counters. A partial wave analysis is made of the experimental results assuming S- and P-wave scattering. The results obtained are $\alpha_3=-4.11\pm1.09$ deg, $\alpha_{33}=3.12\pm0.79$ deg, and $\alpha_{31}=-0.32\pm0.73$ deg.

I. INTRODUCTION

THE scattering of pions by protons has been successfully described within experimental limits over a wide range of energies assuming charge independence and S- and P-wave scattering only. Experimental determinations of the two S-wave phase shifts and the four P-wave phase shifts have been made by many different observers.[1] Orear[2] has shown that most of the existing experimental information on π^++p and π^-+p scattering can be fit by the assumption that $\alpha_{11}=\alpha_{13}=\alpha_{31}=0$, that α_1 and α_3 are linear in pion momentum, η, and that α_{33} is given by a two parameter relation proposed by Chew and Low,[3] which at low energies reduces to an η^3 dependence.

Most of the experiments have been performed in the energy region between 60 Mev and 300 Mev, where the P-wave contribution accounts for most of the observed scattering. From these experiments, the behavior of α_{33} is well established. At 60 Mev,[4] α_1 and α_3 are less than α_{33}. At energies below 60 Mev one may expect from the η dependence that S-wave scattering will become relatively more important and better information on α_3 may be obtained.

At energies below 60 Mev, however, the experimental difficulties are increased by the decreasing pion-proton cross section and the decreasing range of pions in matter. Below 40 Mev, all previous experiments[5] have been performed using cloud chambers or nuclear emulsions. The lowest-energy counter experiment[6] in which differential cross sections have been measured is a CH_2-C difference experiment at 40 Mev. The interpretation of low-energy counter experiments is difficult because of the uncertainty as to what the introduction of hydrogen into the target does to the background. Experiments now in progress at Rochester[7] overcome this difficulty by using a tightly defined geometry to minimize background.

In this experiment, rather than a radical alteration of geometry to eliminate background, an attempt has been made to gain more knowledge of the background by measuring the mass and energy of detected particles by pulse-height analysis. An energy distribution of the background mesons is obtained, from which one is able to determine the number of mesons with sufficiently low energy so that when hydrogen is introduced into the target, the additional ionization loss in hydrogen prevents them from being detected. An estimate of the fraction of these mesons that are actually undetected is obtained from a detailed study of the energy distributions of mesons and a knowledge of the geometry of the experiment. In this manner a correction is obtained for the uncertainty in the background.

II. EXPERIMENTAL PROCEDURE AND RESULTS

The cross sections for 37 ± 4 Mev positive pions scattered in hydrogen have been measured at laboratory angles of 45°, 60°, 90°, 113°, 135°, and 150° to the incident beam. The method used is identical with that used in the experiment reported in the preceding paper[8] on the interactions of positive pions in deuterium. A detailed description of the experimental method is given in that paper.

With the detecting scintillation counter telescope at each angle, alternate runs are taken with the target filled with liquid hydrogen and empty. Before the telescope is moved to a different angle, it is placed at 0° to the incident beam, and a calibration run is taken. Data are obtained in the form of photographs of oscilloscope traces, on each of which are displayed pulsee proportional to the energy lost by particles in the thres counters of the detecting telescope. The data of the experiment consist of these photographs and the incident flux measured by a two-counter scintillation telescope. A total of approximately 25 000 oscilloscope

* This research is supported by the Office of Naval Research and the U. S. Atomic Energy Commission.
† Submitted by B. A. Wooten in partial fulfillment of the requirements for the degree of Doctor of Philosophy in the Faculty of Pure Science, Columbia University.
[1] For a summary of these experiments up to June, 1955, see Schweber, Bethe, and de Hoffmann, *Mesons and Fields* (Row, Peterson and Company, Evanston, 1955).
[2] J. Orear, Nuovo cimento 4, 856 (1956). This paper contains a summary of low-energy pion experiments up to June, 1956.
[3] G. Chew and F. Low, Phys. Rev. **101**, 1570 (1956).
[4] Bodansky, Sachs, and Steinberger, Phys. Rev. **93**, 1367 (1954).
[5] See reference 2 for a summary of the results of these experiments and a bibliography up to June, 1956.
[6] J. P. Perry and C. E. Angell, Phys. Rev. **91**, 1289 (1953).
[7] B. Rose and S. W. Barnes, Bull. Am. Phys. Soc. Ser. II, 2, 195 (1957).
[8] Sachs, Winick, and Wooten, Phys. Rev. **109**, 1733 (1958), preceding paper.

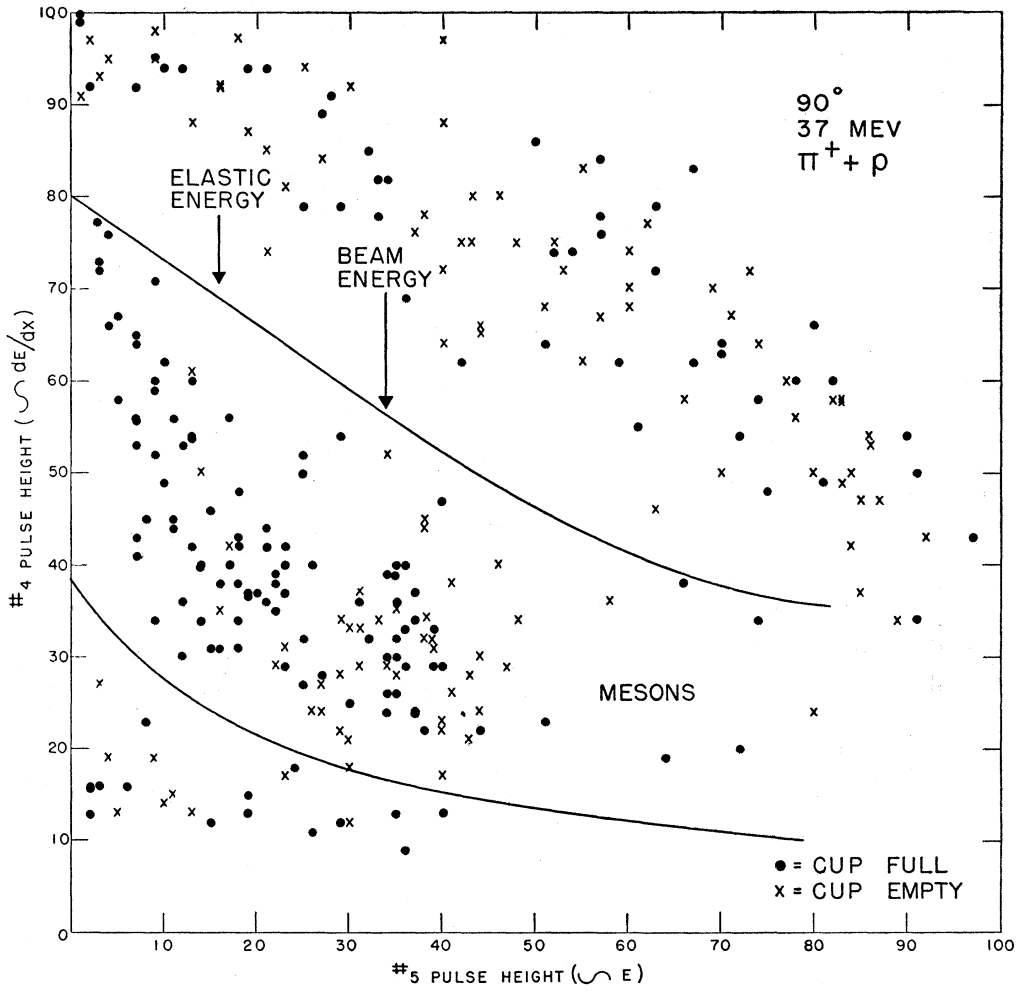

FIG. 1. Typical graph data taken at 90°.

pictures were taken in runs at the six angles, and an equal number of calibration runs.

Figure 1 is a typical example of a graph of these data for a 90° run on which the pulse height in counter 4 (approximately proportional to dE/dx) is plotted *versus* the pulse height in counter 5 (approximately proportional to E) for each oscilloscope picture which does not show an anticoincidence pulse. The data shown in Fig. 1 are for 8.2×10^6 incident mesons with the target filled with liquid hydrogen and for the same incident flux with the target empty.

The solid lines on Fig. 1 that form the boundaries of the meson band are obtained approximately from a calibration run. Points that lie near the boundaries are due to particles that experience a large fluctuation in energy loss in counter 4. The identification of such points is made more certain by the additional knowledge of the pulse height in counter 3, which is an independent measurement of dE/dx.

On the graph, the pulse height in counter 5 corresponding to the median beam energy is indicated and also the pulse height corresponding to the kinematically determined median energy after scattering for the $\pi^+ + p$ process. At 90°, most of the meson background is of full beam energy, principally scattered by the stainless steel and aluminum parts of the target, with very little background in the pulse-height region corresponding to $\pi^+ + p$ scattering. Since mesons of full beam energy (39 Mev) can lose at most 4 Mev in the full 3.1 in. diameter of the hydrogen in the target, the number of particles lost from the background upon introduction of the hydrogen will be negligible.

Points lying above the meson band are background protons from inelastic processes. The ability of the pulse height technique to eliminate protons from the background reduces the running time required to obtain the desired statistical errors. Points below the meson band are mainly accidentals. The anticoincidence counter which is intended to eliminate accidentals, intercepts only 85% of the meson beam. The number of points below the meson band can be entirely accounted for by the 15% inefficiency.

For those particles that do not have sufficient range to give a pulse in counter 5, graphs of pulse height in

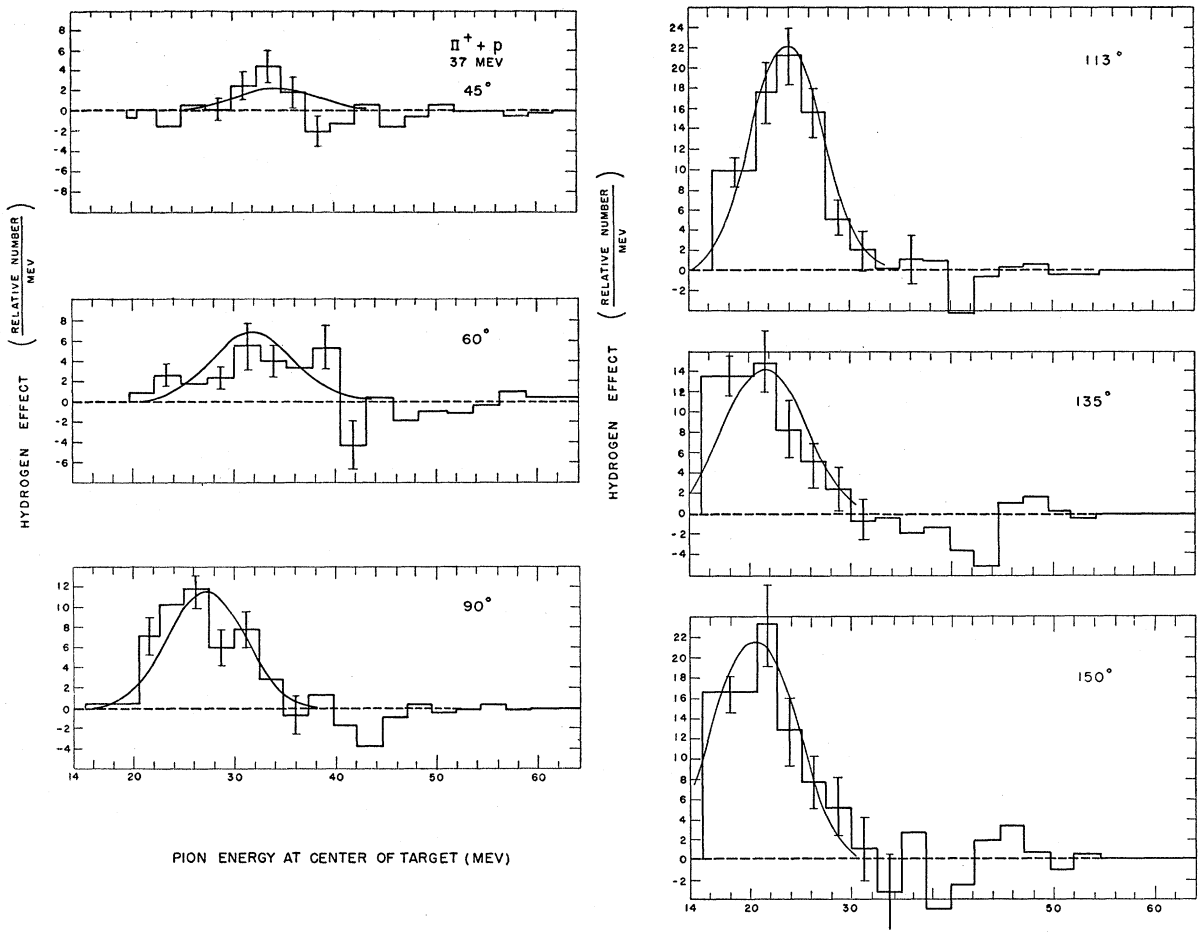

FIG. 2. Energy distributions of positive pions scattered on hydrogen at 45°, 60°, 90°, 113°, 135°, and 150° in the laboratory. The ordinate scale is chosen so that at each angle the area of the histogram is proportional to the differential cross section observed at that angle.

counter 3 *versus* pulse height in counter 4 are made. The energy which a pion must have after scattering at the center of the target in order to reach 5 is 20 Mev. The 3 *vs* 4 graphs extend the low-energy detection threshold of the apparatus to 16 Mev.

The pulse height in counter 5 is calibrated in terms of the energy of a pion after it is scattered at the center of the target, as described in the preceding paper. The histograms shown in Fig. 2 represent the distribution of points in the meson band on the graphs. These histograms are plotted in such a way that the ordinate is proportional to the net number of hydrogen scatterings per Mev per incident pion. The negative effect observed in the nearly elastic energy region of the background at all angles can be accounted for by energy degradation in hydrogen of those pions in the background which pass through the hydrogen before or after scattering in the heavy parts of the target.

On each histogram of Fig. 2 is plotted a predicted distribution, which is obtained in the following manner: The target is divided into 19 cells of equal volume. The emergent energy for a pion of mean beam energy scattered in a given cell at a given angle is computed by considering the energy loss in hydrogen before scattering, the kinematic scattered energy, and the energy loss in hydrogen after scattering. From a consideration of all cells, a predicted emergent energy distribution is obtained for monochromatic incident pions scattered through a given angle. This distribution is then folded into the known beam energy distribution and a Gaussian representing the 6% pulse-height resolution of counter 5 described in the preceding paper. The energy scale adopted for plotting is the energy a pion must have at the center of the hydrogen to emerge with the energy computed above.

The calculated distributions obtained in this way fit the observed hydrogen effect within the statistical errors except at 135°. The 135° histogram is the sum of three independent runs, two of which have a smaller number of pions giving pulses in counter 5 than the distribution predicts, so that the sum of the three does not agree with the distribution. The disagreement may be attributed to a statistical fluctuation.

The distributions are used in this experiment to

TABLE I. Cross sections (in mb/sterad) for $\pi^+ + p$ scattering at 37 Mev.

θ_{lab} / $\theta_{c.m.}$		45° / 53°	60° / 69°	90° / 100°	113° / 123°	135° / 142°	150° / 155°
Uncorrected $(d\sigma/d\Omega)_{lab}$	Run I	0.24 ±0.19	0.49±0.19	0.63±0.15	0.89±0.14	1.19±0.19	1.19±0.24
	Run II	0.11 ±0.16	0.33±0.10	0.53±0.10	0.97±0.10	0.70±0.13	0.98±0.15
Corrected $(d\sigma/d\Omega)_{c.m.}$	Run I	0.19 ±0.15	0.42±0.16	0.65±0.15	1.07±0.17	1.63±0.25	1.81±0.37
	Run II	0.085±0.13	0.28±0.08	0.54±0.10	1.17±0.12	0.95±0.18	1.49±0.23
Weighted mean $(d\sigma/d\Omega)_{c.m.}$		0.13 ±0.10	0.31±0.07	0.57±0.09	1.13±0.10	1.18±0.15	1.58±0.20

compute the fraction of the scattered pions at 135° and 150° that have energies below the threshold of the telescope and are not detected.

III. CALCULATION OF CROSS SECTIONS

A. Experimental Parameters and Laboratory Cross Sections

The laboratory cross sections are computed from the experimental results using the relation and the appropriate parameters given in the preceding paper. The effective density of hydrogen, ρ, is taken to be 4.21×10^{22} atoms per cc, which is the difference between the density of the liquid and the vapor in equilibrium with the liquid at a pressure of 1 atmosphere.

This experiment was performed in two runs. In Run I no anticoincidence technique was used, and the distances between the target, counter 3 and counter 4 were adjusted at each angle to reduce the background. Therefore in Run I the solid angle differed slightly at each angle. In Run II the anticoincidence technique was used, and the standard geometry described in the deuterium experiment[8] was used throughout, giving a solid angle of 0.0344 steradian. The uncorrected laboratory cross sections for the two runs are given in the first two lines of Table I.

B. Corrections to Cross Sections

1. *Low-Energy Threshold of the Telescope*

In this experiment 5% of the incident pions have energies below 33 Mev. Furthermore, at the backward scattering angles some pions will penetrate as much as 0.4 g/cm² of hydrogen, scatter, and then traverse another 0.4 g/cm² of hydrogen before emerging from the target. The number of pions in the scattered beam which are undetected because they have insufficient range after leaving the target is computed from the calculated distributions described above and shown in Fig. 2. The fraction undetected is negligible except at 135°, where it is 4.3%, and at 150°, where it is 8.9%.

2. *$\pi-\mu$ Decay and Multiple Scattering*

The discussion of $\pi-\mu$ decay given in the preceding paper applies equally well to this experiment. The correction to the observed counting rate is calculated to be negligible.

In Run I of this experiment counter 3 was placed closer to the target at some angles than in Run II, where it is kept as close as possible to counter 4. Therefore in Run I the effect of multiple scattering must be considered. A graphical analysis was made under the experimental conditions assuming a Gaussian distribution of particles after multiple scattering. The calculation indicated that in the worst case (150°) 15% of the pions that would have been detected if there were no multiple scattering were scattered out of the telescope, while an almost equal number of pions that would have missed counter 4 were scattered in. The net counting rate calculated was 98% of the counting rate that would be observed if there were no multiple scattering. In view of the small calculated correction and the approximations in the calculation, no correction was made. The principal effect of multiple scattering was shown to be an increase in the width of the angular resolution function of the telescope.

C. Corrected Cross Sections

The laboratory cross sections have been corrected as described above and transformed into the $\pi^+ + p$ center-of-mass system. The results are given in lines 3 and 4 of Table I, together with the statistical errors for Runs I and II. The generally smaller statistical errors in Run II are due to the use of the anticoincidence technique in this run.

The last line of Table I contains the weighted mean differential cross sections in the center-of-mass system. In Fig. 3 these cross sections are plotted *versus* the scattering angle in the center-of-mass system.

IV. DISCUSSION OF RESULTS

Assuming charge independence and only S- and P-wave scattering, the differential cross section for $\pi^+ + p$ scattering in the center-of-mass system is given by the relation[1]

$$\frac{d\sigma}{d\Omega}=\lambda\!\!\!^{-2}\left\{\left(X+Y\cos\theta-\frac{\alpha}{1-\cos\theta}\right)^2+Z^2\sin^2\theta\right\},$$

where $\lambda\!\!\!^{-}$ is the de Broglie wavelength of the incident pion, θ is the scattering angle, α is the phase shift due to the Coulomb potential, and at sufficiently low pion energies $X=\alpha_3$, $Y=2\alpha_{33}+\alpha_{31}$, $Z=\alpha_{33}-\alpha_{31}$.

TABLE II. Phase shifts in degrees for $\pi^+ + p$ scattering at 37 Mev.

	α_3	α_{33}	α_{31}	M	$P-N$
Best fit (±standard deviations)	$-4.11°\pm1.09°$	$3.12°\pm0.79°$	$-0.32°\pm0.36°$	3.47	3
Anderson and Davidon[a]	$-3.85°$	$3.40°$	$-0.73°$	3.72	3
Best fit with α_{31} assumed=0	$-3.86°$	$3.43°$	0	4.92	4
Orear[b] (α_{31} assumed=0)	$-3.95°$	$3.56°$	0	6.92	4

[a] H. L. Anderson and W. C. Davidon, *Proceedings of the Sixth Annual Rochester Conference on High-Energy Nuclear Physics* (Interscience Publishers, Inc., New York, 1956).
[b] See reference 2.

A numerical least squares fit of this relation to the cross sections in Table I has been made. The resulting phase shifts are given in the first line of Table II. For this choice of phase shifts, column 4 of Table II gives the value of the sum $M=\sum(\delta/\epsilon)^2$ (which is minimized), where δ is the difference between the observed and calculated cross section for a given angle, ϵ is the statistical error of the observed cross section and the summation is taken over the experimental angles. Column 5 is the number of experimental points, P, less the number of parameters, N, used for fitting and is equal to the expected mean value of M for a large number of experiments.

In order to make an analysis of the errors, the six second partial derivatives of M with respect to the three phase shifts were evaluated numerically at the best-fit values of the phase shifts. The inverse matrix is found for the symmetrical matrix formed from these partial derivatives. The diagonal elements of the inverse matrix are the standard deviations given in line 2 of Table II. The off-diagonal elements are $\langle\alpha_3\alpha_{33}\rangle=0.835$ deg^2, $\langle\alpha_{33}\alpha_{31}\rangle=-0.0698$ deg^2, and $\langle\alpha_{31}\alpha_3\rangle=-0.0686$ deg^2.

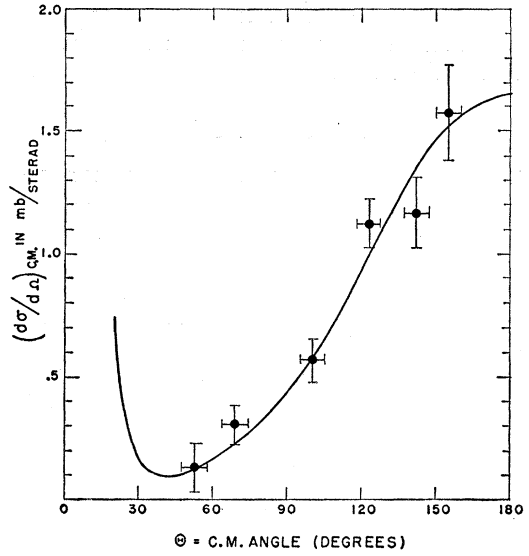

FIG. 3. Differential cross section in the center-of-mass system *versus* center-of-mass angle for $\pi^+ + p \rightarrow \pi^+ + p$ at 37 Mev. The solid curve represents the theoretical cross section for the best-fit values of the phase shifts.

For comparison line 2 contains the phase shifts computed from the semiempirical relations for the phase shifts given by Anderson and Davidon.[9] Line 3 of Table II contains the phase shifts obtained from a least-squares fit for which α_{31} was set equal to zero, so that only two independent parameters were available for fitting. Line 4 contains the phase shifts computed from Orear's extrapolation[2] in which the same assumption is made. It may be seen from column 4 of Table II that the inclusion of α_{31} gives a better fit to the results of this experiment than can be made using α_3 and α_{33} alone. It may also be seen from column 4 that Anderson and Davidon's phase shifts give closer agreement with this experiment than Orear's. However, the experimental errors are sufficiently large that a nonzero value of α_{31} is not required and the experiment cannot be said to be in disagreement with either set of relations for the phase shifts. The curve plotted in Fig. 3 represents the differential cross section computed with the best fit phase shifts of Table II.

ACKNOWLEDGMENTS

We would like to express our appreciation to Miss C. Macleod for her help in scanning photographs and performing calculations, Mr. E. L. Koller and Mr. S. Penman for assistance during experimental runs, Professor E. T. Booth and Mr. D. Koppel for the use of the magnetic channel, and the entire staff of the Nevis Cyclotron Laboratory, especially Mr. R. Parker for preparing the liquid hydrogen.

[9] H. L. Anderson and W. C. Davidon, *Proceedings of the Sixth Annual Rochester Conference on High-Energy Nuclear Physics* (Interscience Publishers, Inc., New York, 1956).